

# Synthesis of ZnO/Au Nanorods for Self Cleaning Applications

Thi Ha Tran<sup>1,2</sup>, Thi Huyen Trang Nguyen<sup>2</sup>, Manh Hong Nguyen<sup>2</sup>, Nguyen Hai Pham<sup>2,\*</sup>, An Bang Ngac<sup>2</sup>, Hanh Hong Mai<sup>2</sup>, Van Thanh Pham<sup>2</sup>, Thanh Binh Nguyen<sup>2</sup>, Khac Hieu Ho<sup>3,4</sup>, Trong Tam Nguyen<sup>5</sup>, and Viet Tuyen Nguyen<sup>2,\*</sup>

<sup>1</sup>Department of Physics, Faculty of Basic Science, University of Mining and Geology, Duc Thang, Tu Liem, Hanoi

<sup>2</sup>Faculty of Physics, VNU-University of Science, Vietnam National University Hanoi, 334 Nguyen Trai, Thanh Xuan, Hanoi

<sup>3</sup>Institute of Research and Development, Duy Tan University, 03 Quang Trung, Hai Chau, Da Nang 550000, Vietnam

<sup>4</sup>Faculty of Natural Sciences, Duy Tan University, 03 Quang Trung, Hai Chau, Da Nang 550000, Vietnam

<sup>5</sup>Department of Physics, Faculty of Basic-Fundamental Sciences, Vietnam Maritime University, 484 Lach Tray – Le Chan – Hai Phong

Zinc oxide (ZnO) is a well-known semiconductor with valuable characteristics: wide direct band gap of  $\sim 3.3$  eV, large exciton binding energy of 60 meV at room temperature, high efficient photocatalyst, etc. which have been applied in many fields such as optical devices (LEDs, laser), solar cells and sensors. Besides, various low dimensional structures of ZnO in terms of nanoparticles, nanorods, nanoneedles, nanotetrapods find applications in technology and life. This material is also appealing due to the diversity of available processing methods including both chemical and physical approaches such as: hydrothermal, sol–gel, chemical vapor deposition and sputtering. In this report, ZnO nanorods are prepared by hydrothermal method assisted with galvanic-cell effect. The effect of counter electrode materials on the morphology and structure of obtained product was studied. Scanning electron microscopy (SEM) images of the product showed that counter electrodes made of aluminum offers nanorods of higher quality than other materials in terms of uniform size, high density and good preferred orientation. The as-prepared nanorods were then sputtered with gold (Au). ZnO/Au nanostructures show excellent photocatalyst activities which were demonstrated by complete photodegradation of methylene blue (Mb) under UV irradiation and high decomposition rate  $k$  of  $0.011 \text{ min}^{-1}$ .

**Keywords:** ZnO/Au Nanorods, Photocatalyst, Hydrothermal Method, Galvanic Effect.

## 1. INTRODUCTION

Zinc oxide (ZnO) is an interesting material, which finds numerous applications from daily life to technology such as: cosmetic, medicine, rubber manufacture, sensors, UV absorber, etc. These applications were developed based on unique properties of ZnO: wide direct bandgap of 3.37 eV at room temperature, piezoelectric properties, chemical stability [1]. Recently, ZnO nanomaterial has attracted more interest from scientists and engineers because many properties of bulk ZnO were enhanced. Hence, nanostructures of ZnO were considered as advanced materials.

ZnO nanorods and nanowires were reported as potential candidates for sensor and spintronics applications.

ZnO is also famous for its good photocatalytic properties thanks to their high surface to volume ratio. Such one-dimensional (1D) nanostructures of ZnO can be obtained by various physical to chemical techniques such as: vapor-liquid–solid [2]; physical deposition [3], microwave irradiation [4], hydrothermal method, etc. [5, 6]. Lately, it was reported that decoration of metal on semiconductor nanostructure can greatly enhance some properties of the intrinsic semiconductors, such as: chemo-resistive property [7], photocatalytic activity [8, 9], photoluminescence [10]. In this paper, we report a simple process to synthesize ZnO nanorods by hydrothermal process assisted with galvanic effect. Even though hydrothermal process assisted with galvanic effect was reported as an efficient method to prepared 1D nanostructures, effect of counter electrode

\*Authors to whom correspondence should be addressed.

material, an important factor of this method was likely not mentioned in previous reports. The effect of counter electrode materials on the morphology and structures of the nanoproducts was studied. Nanocomposite of ZnO and gold (Au) was then prepared by sputtering method. The ZnO/Au nanocomposite showed good photocatalytic properties, which allowed decomposing totally methylene blue (Mb) on the surface of ZnO/Au nanorods after UV treatment. The results showed that ZnO/Au nanorods are promising for making self-cleaning surfaces.

## 2. EXPERIMENTAL DETAILS

ZnO nanorods were prepared on print circuit boards (PCBs) as substrates by hydrothermal process. The detailed experiment setup was described in our previous papers [5, 6]. In a typical process, the native copper oxide layers on substrates were first wiped off using fine sand paper. The substrates were then cleaned thoroughly by ultrasonic bath with ethanol and distilled water several cycles. After that the substrates were blown dried by nitrogen gun. Galvanic effect was used to enhance the growth of ZnO nanorods. Galvanic cell structures were formed by covering edges of the substrate by three different metals indium (In), tin (Sn) and aluminum (Al) to study the effect of cell structures on the nanoproducts. In these structures, the working electrode was the copper (Cu) layer on PCBs and the counter electrode was the other metal: In, Sn and Al and the two electrodes were directly connected. No external power source was applied during synthetic process.

A precursors solution was prepared by mixing solutions of 75 mM zinc nitrate hexahydrate ( $\text{Zn}(\text{NO}_3)_2 \cdot 6\text{H}_2\text{O}$ ) and hexamethylenetetramine ( $\text{C}_6\text{H}_{12}\text{N}_4$ ). Then, the prepared substrates would be dipped horizontally in the as-prepared solution. Temperature of the reaction was kept constant at 90 °C by a temperature controller and reaction time was 3 h. ZnO nanorods would be formed in the opened area in the center of the substrates. Au was sputtered onto ZnO nanorods with a current of 20 mA by a DC sputtering system. The calibration curve for the sputtering system suggested an Au layer of 10 nm would be formed at this synthesis condition. Raman spectra were collected on a Horiba LabRam HR800 Raman spectrometer. The excitation source was a He-Ne laser with the wavelength of 632.8 nm. The structure of the product was studied by X-ray-Bruker D5005 while fluorescence spectra was obtained using a FL-322 spectrometer. The sample morphology was observed by using Electron microscope FEI Nova NanoSEM 450.

Photocatalyst reaction of ZnO/Au nanorods was performed by spraying the substrate with distilled water and treating the sample with ultra-violet (UV) lamp. The emission wavelength of the UV lamp was 290 nm and the power was 1 mW. After photocatalyst reaction, the samples were rinsed with distilled water and blown dry by

nitrogen gun. The existence/decomposition of Mb was checked by surface enhanced Raman scattering.

## 3. RESULTS AND DISCUSSION

ZnO has the wurtzite structure of which space group is  $P6_3mc$ . The group theory states that ZnO has eight phonon modes.  $A_1 + E_1 + 2E_2$  are Raman active,  $2B_2$  are Raman silent, and  $A_1 + E_1$  are IR active [11, 12]. The electric fields induced by LO phonons further splits  $A_1$  and  $E_1$  phonon modes into longitudinal optical (LO) and transverse optical (TO) components.

Raman spectra of the ZnO nanorods synthesized with different counter electrode materials are shown in Figure 1. All the spectra show two dominant characteristic peaks of ZnO at 99 and 437  $\text{cm}^{-1}$ , which can be assigned to  $E_{2L}$  and  $E_{2H}$  modes, respectively [3, 8].

The weak peak at 333  $\text{cm}^{-1}$  can be attributed to the second-order Raman scattering arising from the zone/zero boundary phonons  $E_{2H}-E_{2L}$ , while the Raman peak at 215  $\text{cm}^{-1}$  is assigned to 2TA mode [3]. These two peaks in the Raman spectra imply that ZnO nanorods are oxygen deficient. There is little difference between the spectra of the ZnO nanorods prepared with different counter electrode materials. The results suggested that galvanic effect does not show a clear effect on the structure of nanoproducts.

Figure 2 shows the SEM images of the as-prepared ZnO samples. It can be seen that galvanic effect affects greatly on the morphology of the nanoproduct. As shown in Figure 2, when In and Sn are utilized as counter electrode materials, the density of nanorods is low and the obtained nanorods do not have a preferred orientation. ZnO nanorods prepared with In as counter electrodes are smaller in diameter when compared with the nanorods synthesized with Sn or Al but a large portion of the substrate is

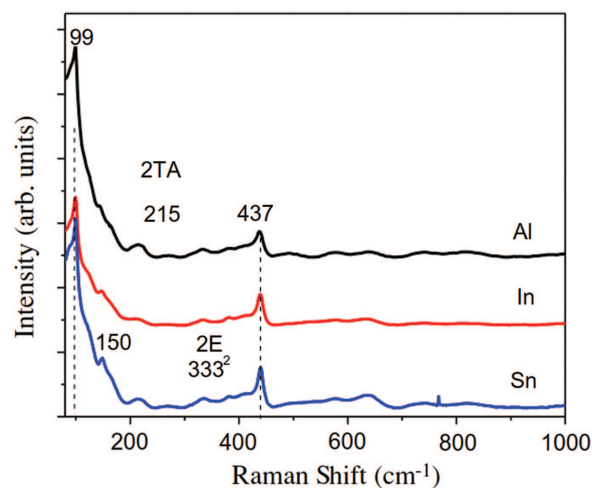


**Figure 1.** Raman spectra of ZnO nanorods prepared with different materials of counter electrodes: Al, In, Sn (data was shifted for better visualization).

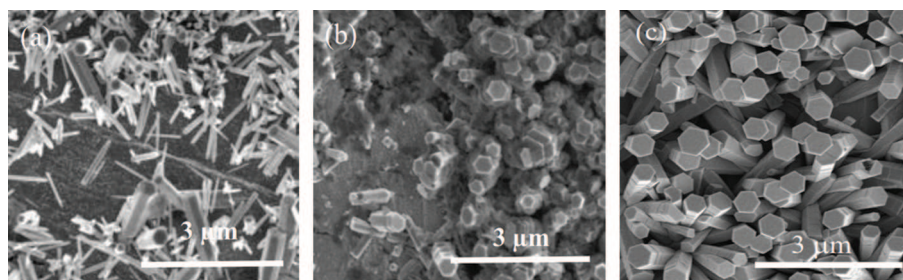


**Figure 2.** SEM images of ZnO nanorods prepared with different materials of counter electrodes: Al, In, Sn.

empty without any nanorods. In the case of Sn, the alignment of nanorods seems to be slightly better but empty area is still large. When compared with In or Sn, Al shows better advantages in term of uniformity and preferred orientation of the nanorods. ZnO nanorods prepared with Al counter electrode have a quite uniform size and morphology. Most of the rods have hexagonal cross-section with diameter of around 300–400 nm and length of 1–2  $\mu\text{m}$ .

The reaction rate was given by equation [13]  $\text{Rate}(\text{mols}^{-1}\text{cm}^{-2}) = j/nF$  where  $F$  is the Faraday constant,  $j$  denotes the current density, and  $n$  is the stoichiometric number of electrons in the electrode reaction. The current density in turn depends on the potential different between electrodes of galvanic structure. Thus changing materials of counter electrodes resulted in different density and morphology of nanoproducs as observed from SEM images. SEM images suggested that ZnO nanorods prepared with Al as counter electrode are uniform and possess good alignment, which are critical for many applications. We further studied the properties of this sample.

XRD pattern of the ZnO nanorods, which were prepared using Al as counter electrode in 3 h at 90  $^{\circ}\text{C}$ , is shown in Figure 3. The pattern matches well with JSPS card No. 36–1451 of ZnO with hexagonal structure. Lattice constants of the samples were estimated as:  $a \approx 0.319 \text{ nm}$ ;  $c \approx 0.521 \text{ nm}$ . The lattice parameters of our sample agree

well with those reported by other groups [12, 14]. Except two peaks of Cu resulted from the substrate, no other peak of impurity or strange phase was observed within XRD detection limit. EDS spectrum of ZnO nanorods sputtered with Au is shown in Figure 4. The spectrum confirms the purity of the sample with only peaks from Zn, O. It should be noted that Cu signal comes from the substrates. Clear peak of Au was observed in the spectrum of ZnO sputtered with Au.

The photocatalytic activity of the prepared ZnO/Au nanorods was studied by Raman spectroscopy. The evolution of Raman signal of Mb, of which initial concentration was  $10^{-6} \text{ M}$ , under UV radiation was observed and the results are shown in Figure 5. These ZnO/Au nanorods show good photocatalytic activity. Figure 5 shows that ZnO/Au nanorods can decompose Mb effectively under UV irradiation. The decomposition of Mb was demonstrated by the gradual decrease of Raman intensity with increasing illumination time. The characteristic Raman peaks of Mb disappear after UV treatment. It is reasonable to consider the concentration of remained Mb is proportional to the Raman intensity. Then, the dependence of Raman intensity upon irradiation time was fitted with pseudo first order model of Langmuir and Hishelwood [15]:

$$\ln \frac{C}{C_0} = -kt$$

where  $C$ ,  $C_0$  are the initial concentration of Mb and concentration of Mb at time  $t$ , respectively and  $k$  is the decomposition rate constant. Fitting process for the strongest Raman peak of Mb at  $1620 \text{ cm}^{-1}$  shows that

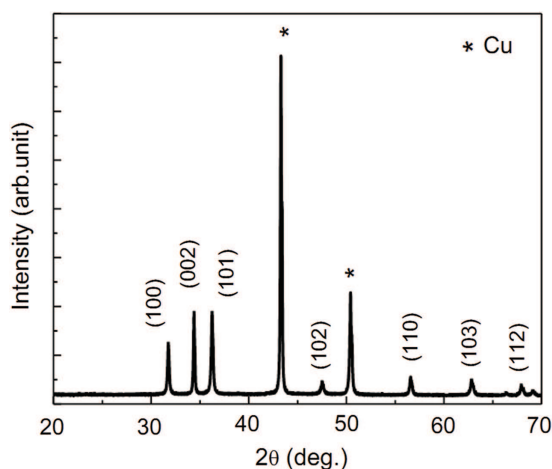


**Figure 3.** XRD patterns of ZnO nanorods prepared with Al as counter electrode in 3 h at 90  $^{\circ}\text{C}$ .

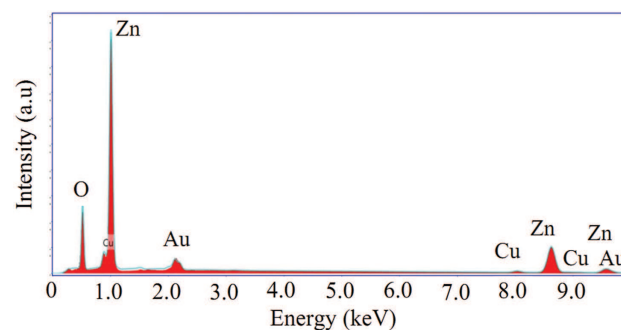


**Figure 4.** X-ray energy dispersive spectrum of ZnO/Au nanorods.

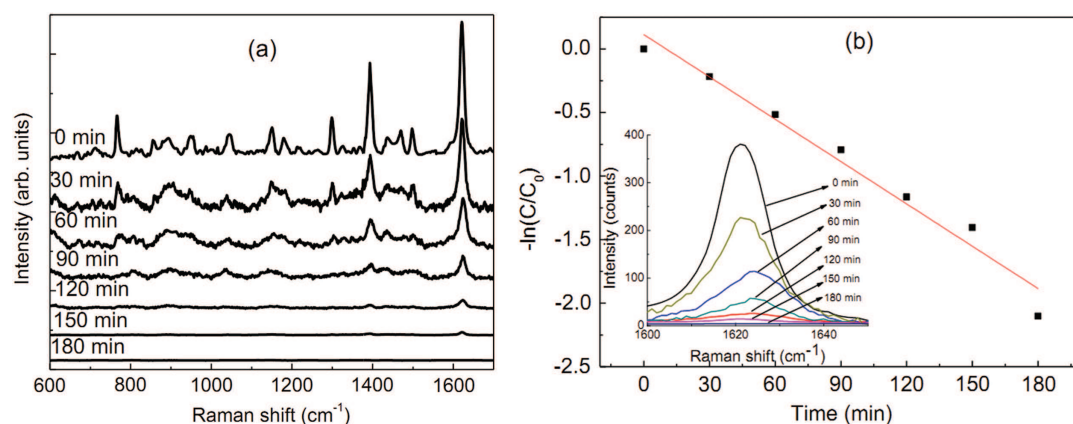


**Figure 5.** (a) Evolution of Raman spectra of Mb on ZnO/Au nanorods under UV irradiation (data was shifted for better visualization), (b) Plot of  $-\ln(C/C_0)$  versus the irradiation time for ZnO/Au nanorods (the inset shows the enlarge Raman peaks of Mb at  $1620\text{ cm}^{-1}$ ).

the decomposition rate of ZnO/Au nanorods in this study is  $k = 0.011\text{ min}^{-1}$ . The decomposition rate of ZnO/Au nanorods is higher than the value reported for ZnO thin films [15, 16], bared ZnO nanoflowers and ZnO nanorods [15].

The self-cleaning ability of ZnO/Au nanorods is resulted from the excellent photocatalytic properties of the ZnO nanorods. Furthermore, the chemical stability of ZnO/Au nanorods [8] guarantees that the self cleaning ability is well preserved. Under UV irradiation, free electrons and free holes are generated. When moving to the surface of ZnO/Au nanorods, these electrons and holes combine with oxygen, water and generate active groups such as:  $\cdot\text{OH}$  and  $\cdot\text{O}_2$ . These active groups will decompose organic compounds into  $\text{CO}_2$  and  $\text{H}_2\text{O}$  [17]. Large surface of the nanorods provides more active sites for photocatalyst reaction and thus resulted in a higher decomposing rate. In addition, it has been reported that better photocatalyst is obtained when ZnO is decorated with noble metal such as Au or Ag [8, 9, 18, 19]. The enhancement is the result of the transfer of electron from ZnO nanorods to Au. This process reduces defect related recombination, which is not beneficial to the photocatalytic ability.

As illustrated in Figure 6, the close Fermi level of Au and defect levels of ZnO facilitates the transfer of electron from ZnO defect states to Au, where Au serves as a reservoir of electron. In the next step, the surface

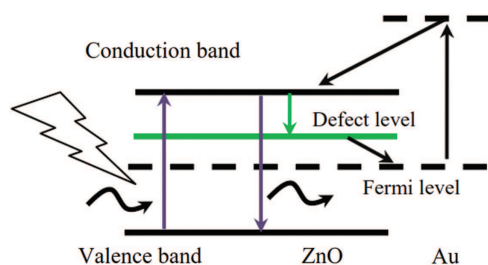


**Figure 6.** Diagram of mechanism for enhancement of band edge emission and green band suppression in ZnO nanorods.

plasmon resonance process provides energy for these electrons to jump up to excited states before transfer back to the conduction band of ZnO. The lower electron density at defect states reduces electron–hole recombination via defect states. At the same time, the number of free electrons and holes necessary for photocatalytic activities gets higher and results in better decomposition efficiency. The combination of high surface area and charge separation of ZnO/Au nanorods explained for the good photocatalyst of our samples.

In order to verify the role of Au in the above discussion on photocatalyst of ZnO/Au nanorods, we performed photoluminescence of bare ZnO nanorods and ZnO/Au nanorods. Figure 7 shows the photoluminescence of the as prepared ZnO nanorods and ZnO/Au nanorods. ZnO has two well known photoluminescence peaks. One corresponds to the near band edge transition, and the other corresponds to the deep levels related to defects in ZnO nanomaterials such as: zinc interstitials or oxygen vacancies. For our sample, the near band edge transition was observed as a sharp peak at 385 nm while the defect

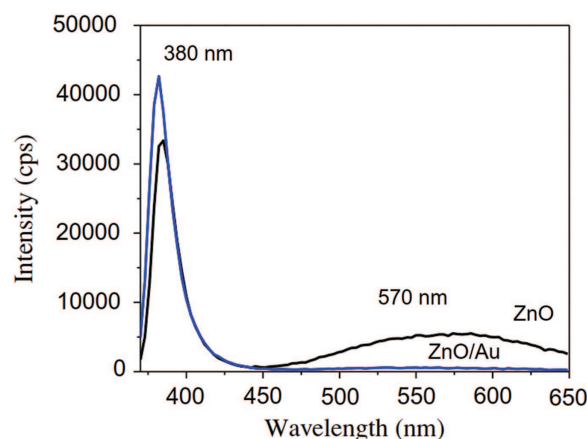


**Figure 7.** Photoluminescence of ZnO nanorods prepared by hydrothermal method assisted with galvanic effect and ZnO/Au nanorods.



related transitions are characterized by a broad band in the region 570 nm. For photocatalyst activity, these defect transitions might not be useful because they reduce the number of free electrons and holes which are necessary for photocatalyst. It can be seen clearly from Figure 7 that the green band related to defect emission in ZnO was completely suppressed after Au sputtering process. Simultaneously, the band to band emission was strengthened clearly. Photoluminescence data likely supported the suggested mechanism (Fig. 6) for photocatalyst of ZnO/Au nanorods.

#### 4. CONCLUSION

ZnO/Au nanorods were successfully synthesized by galvanic assisted hydrothermal and sputtering method. The results show that counter electrode material shows clear effect on the density and morphology of the obtained nanorods. Among the studied materials, Al was the best choice for counter electrode, which offers ZnO nanorods of uniform size and shape with good orientation. The obtained nanorods have uniform size of 200–300 nm in diameter and 1–2  $\mu\text{m}$  in length with hexagonal cross-section. The samples show good photocatalyst with ability to decompose completely Mb absorbed on the surface of the samples at a high decomposition rate of  $0.011\text{ min}^{-1}$ . The mechanism for good catalyst of the product was suggested as the combination of high efficiency of electron hole pair generation under UV irradiation due to high surface area of the nanorods and charge transfer between ZnO nanorods and Au sputtered on the surface of ZnO nanorods.

**Acknowledgments:** This research is funded by the Vietnam National University, Hanoi (VNU) under project number QG.18.17. One of the author, Ph.D. student Thi Ha Tran, would like to thank the Domestic Master/Ph.D. Scholarship Programme of Vingroup Innovation Foundation for supporting tuition fee.

#### References and Notes

- Fabbri, B., Gaiardo, A., Giberti, A., Guidi, V., Malagù, C., Martucci, A., Sturaro, M., Zonta, G., Gherardi, S. and Bernardoni, P., **2016**. Chemoresistive properties of photo-activated thin and thick ZnO films. *Sensors Actuators, B Chem.*, 222, p.1251.
- Hoa, T.T.Q., Canh, T.D., Long, N.N., Tuyen, N.V. and Phuong, N.D., **2017**. Photoluminescence of ZnO nanostructure prepared by catalyst-assisted vapor-liquid-solid technique. *ASEAN J. Sci. Technol. Dev.*, 24, p.131.
- Tuyen, N.V., Long, N.N., Hoa, T.T.Q., Nghia, N.X., Chi, D.H., Higashimine, K., Mitani, T. and Canh, T.D., **2009**. Indium-doped zinc oxide nanometre thick disks synthesised by a vapour-phase transport process. *J. Exp. Nanosci.*, 4, p.243.
- Ha, T.T., Canh, T.D. and Tuyen, N.V., **2013**. A quick process for synthesis of ZnO nanoparticles with the aid of microwave irradiation. *ISRN Nanotechnol.*, 2013, p.1.
- Van Thanh, P., Nhu, L.T.Q., Mai, H.H., Tuyen, N.V., Doanh, S.C., Viet, N.C. and Kien, D.T., **2017**. Zinc oxide nanorods grown on printed circuit board for extended-gate field-effect transistor pH sensor. *Journal of Electronic Materials*, 46, p.3732.
- Mai, H.H., Pham, V.T., Nguyen, V.T., Sai, C.D., Hoang, C.H. and Nguyen, T.B., **2017**. Non-enzymatic fluorescent biosensor for glucose sensing based on ZnO nanorods. *Journal of Electronic Materials*, 46, p.3714.
- Gaiardo, A., Fabbri, B., Giberti, A., Guidi, V., Bellutti, P., Malagù, C., Valt, M., Pepponi, G., Gherardi, S., Zonta, G., Martucci, A., Sturaro, M. and Landini, N., **2016**. ZnO and Au/ZnO thin films: Room-temperature chemoresistive properties for gas sensing applications. *Sensors Actuators, B Chem.*, 237, p.1085.
- Doan, Q.K., Nguyen, M.H., Sai, C.D., Pham, V.T., Mai, H.H., Pham, N.H., Bach, T.C., Nguyen, V.T., Nguyen, T.T., Ho, K.H. and Tran, T.H., **2019**. Enhanced optical properties of ZnO nanorods decorated with gold nanoparticles for self cleaning surface enhanced Raman applications. *Applied Surface Science*, 144593, DOI: 10.1016/j.apsusc.2019.144593.
- Unlu, I., Soares, J.W., Steeves, D.M. and Whitten, J.E., **2015**. Photocatalytic activity and fluorescence of gold/zinc oxide nanoparticles formed by dithiol linking. *Langmuir*, 31, p.8718.
- Cheng, C.W., Sie, E.J., Liu, B., Huan, C.H.A., Sum, T.C., Sun, H.D. and Fan, H.J., **2010**. Surface plasmon enhanced band edge luminescence of ZnO nanorods by capping Au nanoparticles. *Applied Physics Letters*, 96, p.1.
- Bian, H.Q., Ma, S.Y., Zhang, Z.M., Gao, J.M. and Zhu, H.B., **2014**. Microstructure and Raman scattering of Ag-doping ZnO films deposited on buffer layers. *Journal of Crystal Growth*, 394, p.132.
- Zeferino, S.R., Flores, B.M. and Pal, U., **2011**. Photoluminescence and raman scattering in ag-doped zno nanoparticles. *J. Appl. Phys.*, 109(1), p.014308.
- Yang, C.J., Tsai, D.Y., Chan, P.H., Wu, C.T. and Lu, F.H., **2013**. Hydrothermal-galvanic couple synthesis of directionally oriented BaTiO<sub>3</sub> thin films on TiN-coated substrates. *Thin Solid Films*, 542, p.108.
- Zonta, G., Astolfi, M., Casotti, D., Cruciani, G., Fabbri, B., Gaiardo, A., Gherardi, S., Guidi, V., Landini, N., Valt, M. and Malagù, C., **2020**. Reproducibility tests with zinc oxide thick-film sensors. *Ceramics International*, 46, p.6847.
- Di Mauro, A., Fragalà, M.E., Privitera, V. and Impellizzeri, G., **2017**. ZnO for application in photocatalysis: From thin films to nanostructures. *Materials Science in Semiconductor Processing*, 69, p.44.
- Vallejo, W., Cantillo, A. and Díaz-Urbe, C., **2020**. Methylene blue photodegradation under visible irradiation on Ag-doped ZnO thin films. *Int. J. Photoenergy*, 2020, p.1.
- Chen, X., Wu, Z., Liu, D. and Gao, Z., **2017**. Preparation of ZnO photocatalyst for the efficient and rapid photocatalytic degradation of Azo dyes. *Nanoscale Res. Lett.*, 12, p.4.
- El-Bindary, A.A., El-Marsafy, S.M. and El-Maddah, A.A., **2019**. Enhancement of the photocatalytic activity of ZnO nanoparticles by silver doping for the degradation of AY99 contaminants. *Journal of Molecular Structure*, 1191, p.76.
- Li, P., Wei, Z., Wu, T., Peng, Q. and Li, Y., **2011**. Au–ZnO hybrid nanopyramids and their photocatalytic properties. *Journal of the American Chemical Society*, 133, p.5660.

Received: 31 December 2019. Accepted: 22 July 2020.